Annals of Biomedical Engineering, Vol. 24, pp. 222–233, 1996
Printed in the USA. All rights reserved.

0090-6964/96 $10.50 + .00

The Electrical and Dielectric Properties of Human Bone Tissue and Their Relationship with Density and Bone Mineral Content

PAUL ALLEN WILLIAMS* and SUBRATA SAHA†

*Department of Orthopaedic Surgery, Loma Linda University School of Medicine, Loma Linda, CA, and †Marlan and Rosemary Bourns College of Engineering, University of California, Riverside, CA

Abstract—In this study, we examined the electrical properties of wet human cortical and cancellous bone tissue from distal tibia and their relationship to the wet, dry, and ash tissue densities. The resistivity and specific capacitance of both cortical and cancellous bone were determined for different frequencies and directions (orientation). The wet, dry, and ash tissue densities of the bone samples were measured, and the ash content was determined. Correlation and regression analysis was used to examine the possible relationships among the electrical properties and the tissue densities for cancellous and cortical bone specimens separately as well as for all of the bone specimens combined. Highly significant positive correlations ($p < 0.001$) were found between the wet density of bone and the dry and ash densities. The specific capacitance of the cancellous bone specimens in all three orthogonal directions showed significant ($p < 0.01$) positive correlations with the wet, dry, and ash densities. In general, the specific capacitance depended more on density for all bone specimens, and only a weak relationship was found between the resistivity of human cortical bone and density.

Keywords—Electrical properties, Human bone, Density, Resistance, Capacitance.

INTRODUCTION

Since the early 1970s, electrical stimulation has been used by orthopedic surgeons for the treatment of nonunions and congenital pseudoarthrosis (1–3,21,29,45). Both direct current stimulation by means of implanted electrodes (3,21) and induced stimulation by means of external coils (1,2,5,11) have been used. In addition, capacitively coupled stimulation has been demonstrated as a possible treatment methodology (4). Recently, electrical stimulation also has been suggested as a possible treatment modality for osteoporosis, (4,37,49) and for enhanced healing of massive bone grafts after bone tumor resections (5).

Acknowledgment—This work was supported in part by the National Science Foundation Grant No. ECS-8312680.

Presented in part at the 13th Annual IEEE EMBS Conference held in Orlando, Florida, Oct. 31–Nov. 3, 1991, and at the 14th Annual Meeting of the Society for Physical Regulation in Biology and Medicine held in Arlington, Virginia, Oct. 13–16, 1994.

Address correspondence to S. Saha, Marlan and Rosemary Bourns College of Engineering, University of California, Riverside, CA 92521, U.S.A.

(Received 27Sep95, Revised 17Nov95, Accepted 22Nov95)

However, the transduction mechanisms of these treatment modalities and the stimulation parameters necessary for obtaining the maximum clinical effectiveness are not widely known (46). If we can characterize the electric field and current distributions in bone resulting from direct and induced electrical stimulation, then it will be possible to develop a better understanding of the role of electrical stimulation in bone remodeling (10,16). As a first step toward developing a model for estimating the current distribution in bone, we need accurate data on the electrical properties of both cortical and cancellous bone and the factors that influence them (10,29). Several investigators have measured the electrical and dielectric properties of cortical bone (8,9,13–15,17,25–28,34,41,46). Most of these studies were conducted *in vitro*, because *in vivo* impedance measurements do not provide accurate data regarding the electrical material properties because of the irregular geometry and inhomogeneous structure of bone (48). Therefore, *in vitro* measurements have been performed by us and other investigators on standardized bone specimens to determine the dielectric properties of bone tissue. However, one of the difficulties in determining the dielectric properties of any biological tissue is that many factors may affect the impedance measurement in an *in vitro* experiment (37,48). These factors can result in measurements that are significantly different from *in vivo* bone properties (48). Many early authors measuring electrical properties of bone used bone tissue from animals, such as the rat or cow, or used human bone material that was dried or allowed to dry and then rehydrated (35,48). It has been shown that rehydration may not fully restore the original moisture content of bone, and this affects its measured bone properties (48). Moreover, the dielectric properties of human bone tissue may differ from those of animal bone tissues (25). Many factors, such as moisture content, fluid conductivity, and the frequency of measurement, have been demonstrated to affect the electrical behavior of bone tissue (9,26,34) and these have been described in detail by Saha *et al.* (38) and Singh and Saha (48).

Most whole bones are composed of the cortical or compact outer shell, the porous cancellous or trabecular portion, the marrow and other tissues filling the pores of the cancellous, and to some extent the cortical bone (19,23).

TABLE 1. Details of the below-knee amputation specimens.

Specimen	Sex	Bone Type	Age (years)	Diagnosis
1	M	Cancellous	71	Peripheral vascular disease of right leg
2	F	Cancellous	60	Gangrene of right foot
3	M	Cancellous and cortical	54	Gangrene of left foot

Information is available regarding the electrical properties of cortical bone, (48) with limited information for cancellous bone (40) and bone marrow (50). De Mercato and Garcia-Sanchez (13,14) have shown that, for bovine bone, the electrical and dielectric properties vary with the location of the sample and the properties of cortical bone differs from those of cancellous bone. Previously we have measured the electrical and dielectric behavior of wet human cortical and cancellous bone from distal tibiae (40–42). In these previous studies, data were presented on the frequency dependence of the electrical and dielectric properties of cortical and cancellous bone. In addition, some preliminary data were presented concerning relationships among the properties in the longitudinal direction and the transverse directions, as well as relationships among the electrical and dielectric properties and the tissue densities (40–42). The relationship between the mechanical properties of bone and its physical properties (densities) has been investigated in detail (6,7,20,23,24). It has been established that the cortical and the cancellous bone tissue can be considered mechanically as one material with varying densities (7,20,23,24). Although this does not negate the role of microstructure, densities can be obtained from computed tomography (CT) data. This relationship can be used in determining the material properties of *in vivo* bone for finite element models (FEM) used in biomechanical studies (22). To understand the electric field and current distributions in bone under *in vivo* conditions, it is necessary to estimate the electrical properties for different regions and for each portion (cortical, cancellous, and marrow) of the whole bone. This could aid in the development of appropriate models for simulating the field and current distributions and determining interfacial effects among the cortical bone, the cancellous bone, and the marrow (10). Because the density at any point in a bone can be determined noninvasively with CT methods, the development of an *in vivo* electrical model of bone would be facilitated if a relationship were established between the tissue density and the electrical properties of the bone. In addition, such information could be useful in the development and interpretation of electrical impedance tomography and other noninvasive techniques (53,54).

Therefore, the objective of this work was to examine the possible relationships among the electrical properties and tissue densities for both human cortical and cancellous bone. A pulsing electromagnetic field can contain a wide range of frequencies; so measurements at various frequencies were made and the relationships investigated for different frequencies. Other investigators have shown that the electrical properties are dependent on the direction of the measurement and orientation of the sample. Therefore, measurements were made in all three principal directions.

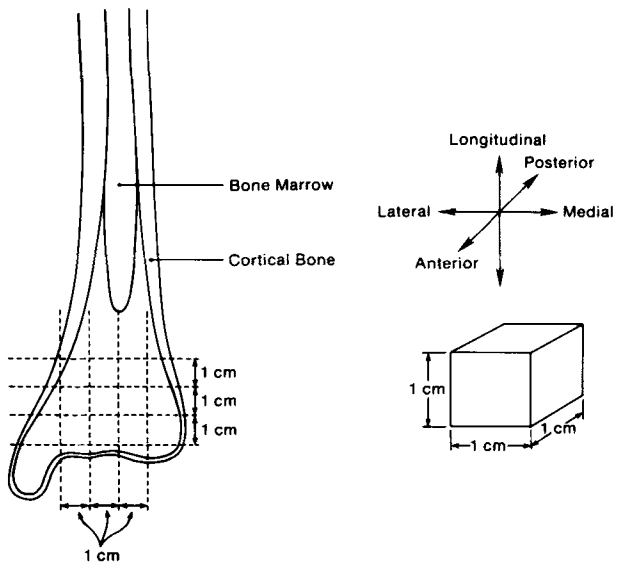

FIGURE 1. Diagram of distal tibia and the machined cancellous bone sample.

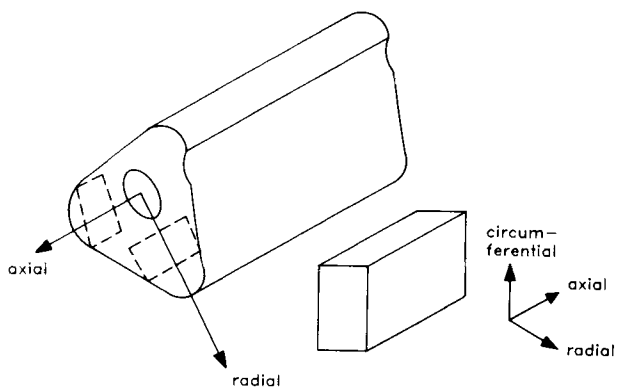

FIGURE 2. Diagram of distal tibia section and the machined cortical bone sample.

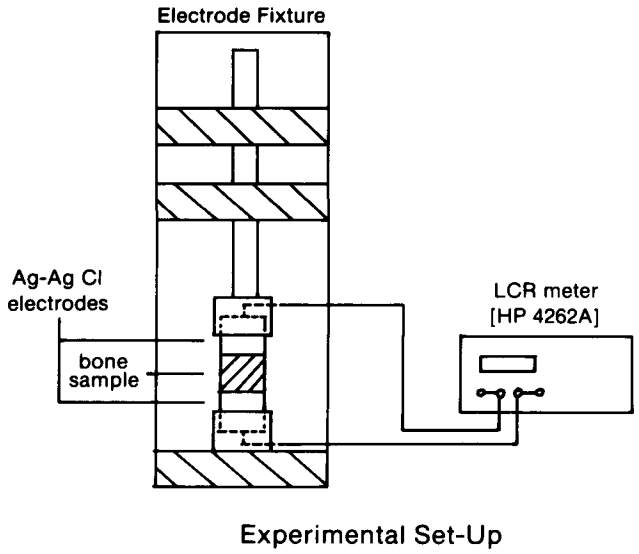

FIGURE 3. Schematic of the measurement setup.

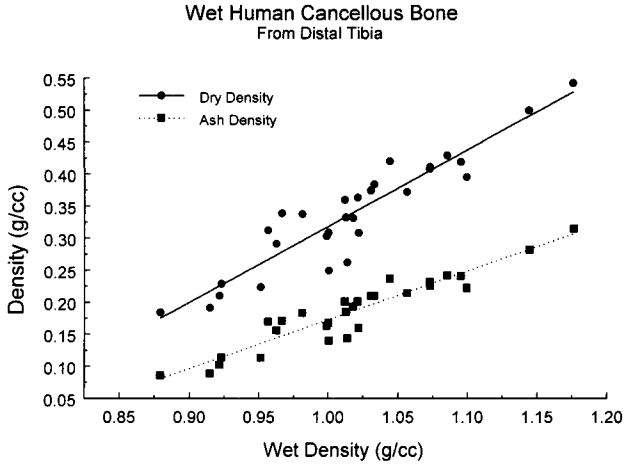

FIGURE 4. Dry density (ρ_{dry}) and ash density (ρ_{ash}) as a function of the wet density (ρ_{wet}) for the cancellous bone specimens.

MATERIALS AND METHODS

Sample Preparation

Three tibiae were obtained from below-knee amputation specimens of three African-American patients. Details of each of these tibia specimens are shown in Table 1. The specimens were obtained shortly after pathological examination and had been maintained under refrigeration from post-surgery until examination. All of the soft tissue was removed, and the bones were wrapped in cotton towels soaked in lactated Ringer's solution and placed in plastic bags, which were then sealed. For specimens 2 and 3, the gangrene was localized at the distal tip of the foot, and the tibiae appeared to be normal. The specimens were stored in a freezer at -10 to -20°C until they were machined.

The whole bone specimens were machined to prepare standardized samples. The bone samples were kept moist with water irrigation throughout the machining process. Cancellous bone specimens that were approximately 1 cm $\times$ 1 cm $\times$ 1 cm (1 cm^3) were machined from the distal portion of each tibia by using the scheme shown in Fig. 1. Details of the machining process have been previously described (40). A total of 30 1 cm^3 cancellous bone samples, 10 from each tibia, were used for the electrical measurements. In addition, 10 cortical bone samples were machined from specimen 3 (Table 1). Five sections that were approximately 1- to 1.5-cm long were cut from the distal third of the tibia. From these sections, 10 rectangular cortical bone samples that were approximately 1–1.5 cm in the axial direction, 0.5–1 cm in the circumferential direction, and 0.4–0.7 cm in the radial direction were machined. As shown in Fig. 2, the samples were machined so that the two transverse faces (radial and circumferential) were flat smooth surfaces correctly oriented with respect to the long axis of the bone (41). All specimens were cleaned in an ultrasonic cleaner to remove any surface debris, maintained in lactated Ringer's solution (pH, 6.5) with an antibacterial agent, and marked so that the orientation was known (40,41). The samples were placed in the humidity chamber (27°C at approximately 100% relative humidity) immediately after preparation. The chamber and samples were allowed to equilibrate overnight before measurements were made.

Electrical Measurements

Figure 3 shows the experimental setup used in measuring the electrical properties of the bone specimens that were tested in all three directions (longitudinal, anterior-posterior, and lateral-medial for the cancellous bone and axial, circumferential, and radial for the cortical bone). Other authors have shown that the dielectric properties of bone vary as a function of moisture content (36,38).

TABLE 2. Physical properties (mean ± SD) of cancellous and cortical bone samples.

	Apparent Density (g/cc)			Ash Content (% of dry wt.)
	Wet	Dry	Ash	
Cancellous (n = 30)	1.018 ± 0.068	0.336 ± 0.087	0.184 ± 0.055	54.2 ± 3.2
Cortical (n = 10)	1.857 ± 0.043	1.579 ± 0.053	1.059 ± 0.050	67.0 ± 1.1

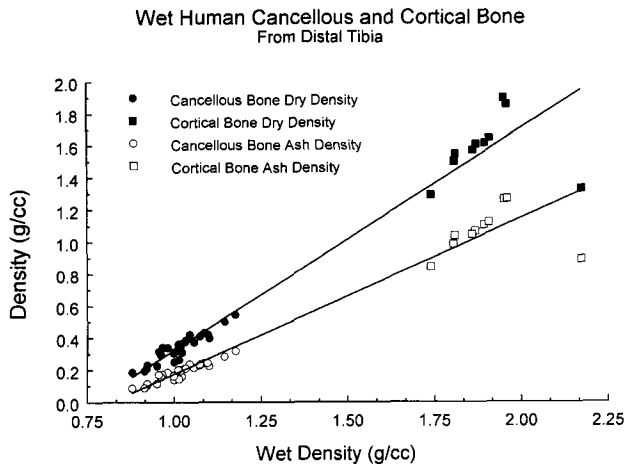

FIGURE 5. Dry density (ρ_{dry}) and ash density (ρ_{ash}) as a function of the wet density (ρ_{wet}) for the cancellous and cortical bone specimens combined.

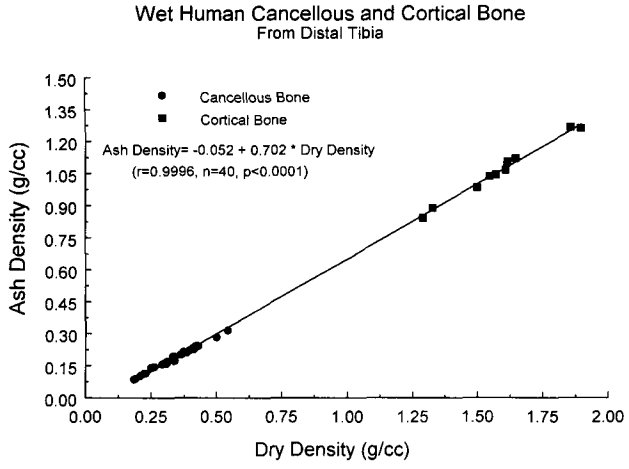

FIGURE 7. Ash density (ρ_{ash}) as a function of dry density (ρ_{dry}) for cancellous and cortical bone specimens combined.

Therefore, measurements were made at a temperature of 27°C in a humidity chamber at near 100% relative humidity to prevent moisture loss during testing. Chlorided-silver metal electrodes, 1.5 cm in diameter, were used for the electrical measurement of the specimens (38,40,41). The resistance and the capacitance in all three directions were measured at frequencies of 10 kHZ, 100 kHZ, and 1 MHZ by using a multifrequency LCR meter (Hewlett Packard 4275A, Hewlett Packard, Englewood, CA). The properties in the longitudinal or axial direction also were measured at frequencies of 120 HZ, 1 kHZ, 20 kHZ, 40 kHZ, 200 kHZ, 400 kHZ, 2 MHZ, 4 MHZ, and 10 MHZ. A second LCR meter (Hewlett Packard 4262A) was used for the measurements at 120 HZ and 1 kHZ. Electrode artifacts, in particular, those at the lower frequencies (<10 kHZ) have been shown previously to not be significant for the electrodes used (38,40,41).

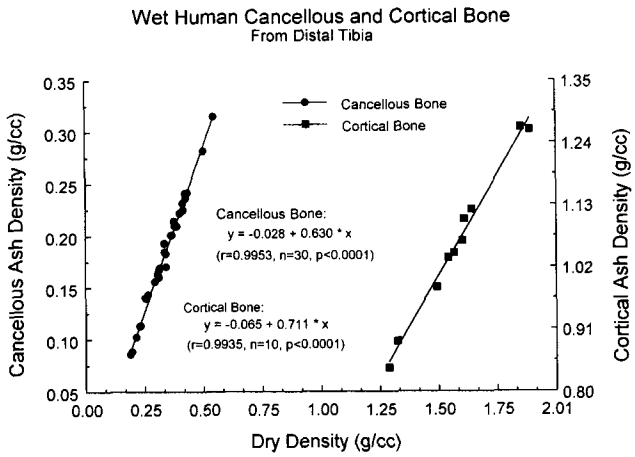

FIGURE 6. Ash density (ρ_{ash}) as a function of dry density (ρ_{dry}) for cancellous and cortical bone specimens.

Physical Properties

After the electrical properties and the dimensions of the specimens were measured, their wet weight was determined by using a balance (Sartorius 2434, Sartorius, Bohemia, NY). All specimens then were cleaned in a solution of acetone in an ultrasonic cleaner (Bransonic 220, Branson Ultrasonics Corp., Danbury, CT) for 1 hr, then the acetone was changed, and the specimens were placed back into the ultrasonic cleaner for 1 additional hr. Subsequently, the specimens were dried in a desiccator overnight, and then further dried in a vacuum oven (Fisher Isotemp 281, Fisher Scientific, Pittsburgh, PA) at 100°C for 1 hr in a vacuum. Then, the samples were weighed in aluminum weighing pans to obtain the dry weight. Finally, the samples were ashed in a laboratory box furnace (Lindberg 51894, Lindberg, Watertown, WI) for no less than 4 hr at 550°C, and the ash weight was measured. From these measurements, the wet, dry, and ash densities were calculated. All densities were calculated in terms of the overall sample volume.

Data Analysis

The values of the various electrical and dielectric parameters were calculated by using the following procedure and equations. The resistivity (R_{sp}) and specific capacitance (C_{sp}) were calculated by using the following relations:

$$R_{sp} = R * A/d \quad (1)$$

$$C_{sp} = C * d/A \quad (2)$$

where R and C are the measured resistance and capacitance of the specimen, respectively, A is the cross-sectional area of the measured surface, and d is the thickness of the specimen in the direction of measurement. Regression analysis was performed to examine the relationships among the electrical properties of bone and the

TABLE 3. Linear regression results of the relationships among the wet, dry, and ash densities for the cancellous (n = 30) and cortical (n = 10) bone specimens.

X	Bone	b Intercept	m Slope	r Value	p Value	Fig.
ρ_{wet} *versus* ρ_{dry}	Cancellous	−0.870	1.190	0.9274	<0.0001	4
ρ_{wet} *versus* ρ_{ash}	Cancellous	−0.590	0.763	0.9409	<0.0001	4
ρ_{wet} *versus* ρ_{dry}	Combined	−1.063	1.385	0.9766	<0.0001	5
ρ_{wet} *versus* ρ_{ash}	Combined	−0.799	0.973	0.9772	<0.0001	5
ρ_{dry} *versus* ρ_{ash}	Cancellous	−0.028	0.630	0.9953	<0.0001	6
ρ_{dry} *versus* ρ_{ash}	Cortical	−0.065	0.711	0.9935	<0.0001	6
ρ_{dry} *versus* ρ_{ash}	Combined	−0.052	0.702	0.9996	<0.0001	7

tissue densities. Because the relationship between the mechanical properties and the densities has been shown to be a power law relation, (6,7) we investigated both linear and power function regressions in analyzing our data.

RESULTS

Physical Properties

Table 2 shows the means and standard deviations for the wet, dry, and ash densities (ρ_{wet}, ρ_{dry}, and ρ_{ash}, respectively). As can be seen in Table 2, there were small variances in the tissue densities. The percent ash contents of the dry weight of 54.2% for the cancellous bone and 67.0% for the cortical bone compare well with those of 56.2% and 63.1%, respectively, obtained by Gong *et al.* (18). These results have been discussed previously (40,41). Figure 4 shows the relationships among the dry, ash, and wet densities for the cancellous bone specimens. Figure 5 shows the relationships among the dry, ash, and wet densities for the cancellous and cortical bone specimens combined. Figures 6 and 7 show the relationship between the dry and ash densities for the cancellous and cortical bone specimens. Figure 6 show this separately for the cancellous and cortical bone. In Fig. 6, it is shown that the two lines are similar; therefore, the cancellous and cortical bone samples were pooled, and a linear regression analysis was conducted for all of the specimens, which resulted in the graph shown in Fig. 7. Table 3 lists all of the regression results for Figs. 4–7. The slopes for the relationships between the dry and ash densities are given in Table 3 are 0.63 for the cancellous bone and 0.711 for the cortical bone. These values, when expressed as percentages, are 63% and 71.1%, which, when compared with the ash contents shown in Table 2, differ by 16.2% for the cancellous bone and 6.1% for the cortical bone. Keyak *et al.* (24) have reported a value of 59.7% for the regression slope between the dry and ash densities. This is a difference of 3.3%, however, their data was for proximal tibial cancellous bone, whereas our data was for distal tibial cancellous bone (24). In both studies, r values of 0.995 and 0.996 were found.

Electrical Properties as a Function of Density

No significant correlations existed between the densities and the resistivity of the cancellous bone sample; how-

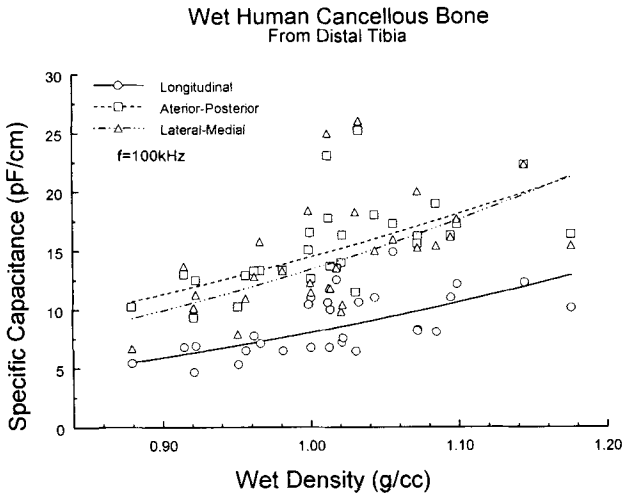

FIGURE 8. The specific capacitance (C_{sp}) as a function of wet density for the longitudinal, anterior-posterior, and lateral medial directions at a frequency of 100 kHZ.

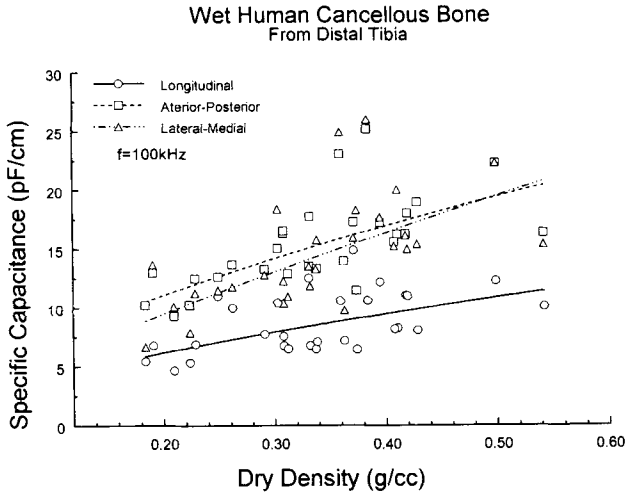

FIGURE 9. The specific capacitance (C_{sp}) as a function of dry density for the longitudinal, anterior-posterior, and lateral medial directions at a frequency of 100 kHZ.

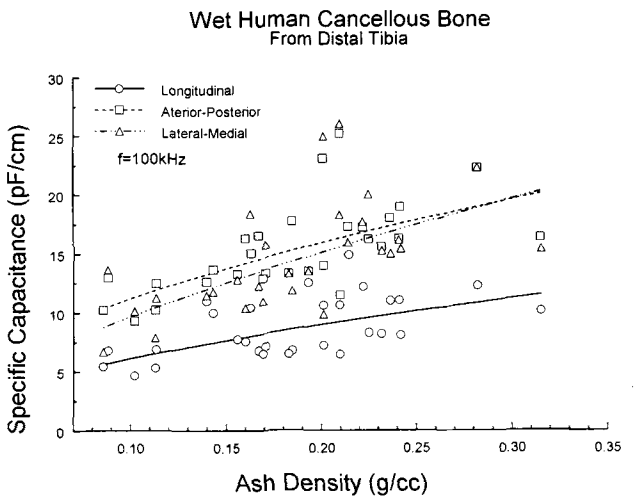

FIGURE 10. The specific capacitance (C_{sp}) as a function of ash density for the longitudinal, anterior-posterior, and lateral medial directions at a frequency of 100 kHZ.

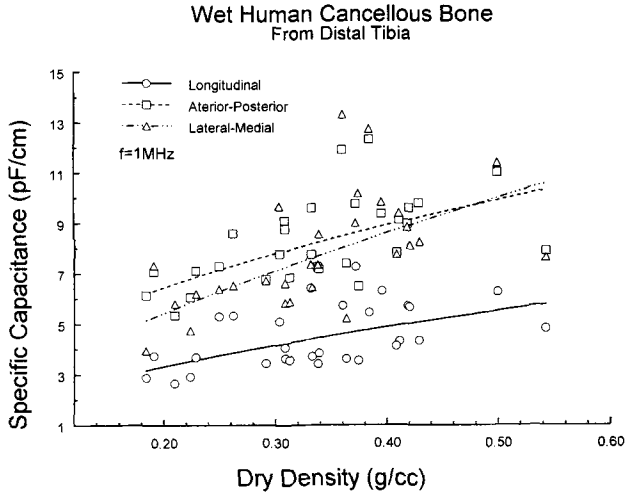

FIGURE 12. The specific capacitance (C_{sp}) as a function of dry density for the longitudinal, anterior-posterior, and lateral medial directions at a frequency of 1 MHZ.

ever, statistically significant positive correlations were found between the densities and the specific capacitance. The relationships between the densities and the specific capacitance for the cancellous bone samples are shown in Figs. 8–13 along with the linear regression lines. The coefficients for the linear regression lines are described in Tables 4 and 5. Similarly, the coefficients for the power regression results are shown in Tables 6 and 7. The general equations are of the form

$$C_{sp} = b + m*\rho \quad \text{(linear)}$$

$$C_{sp} = a*\rho^{\alpha} \quad \text{(power)}$$

where C_{sp} is the specific capacitance, a and b are constants, ρ is the density, m is the linear slope, and α is the exponential power. Although the power-fit curves are not shown in Figs. 8–13, the figures do show the data points used in the regression. It can be seen from Tables 4–7 that, in general, the power-fit equations have a higher r value and a lower p value than do the linear equations. Tables 6 and 7 show the exponential values of 1.9–2.94 for the wet density, 0.47–0.78 for the dry density, and 0.39–0.64 for the ash density. Carter and Hayes (6,7) found that the compressive strength was related to the square of the density, and the strain rate was related to the 0.06 power. Analogously, strain rate and frequency are both time rate of change phenomena, on which the mechanical and electrical properties, respectively, are dependent. Therefore, we examined the specific capacitance as a function of both

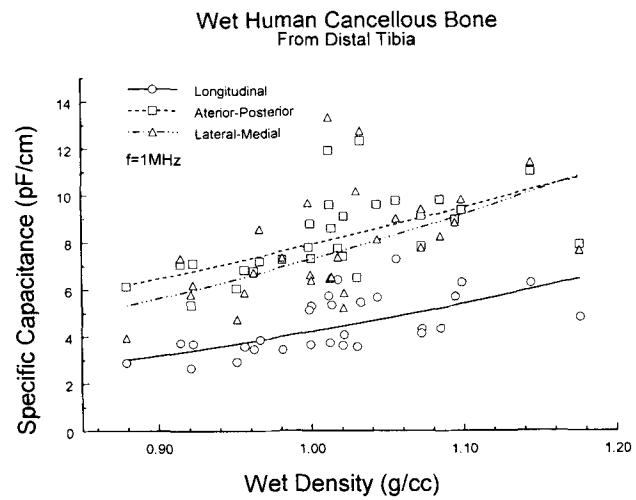

FIGURE 11. The specific capacitance (C_{sp}) as a function of wet density for the longitudinal, anterior-posterior, and lateral medial directions at a frequency of 1 MHZ.

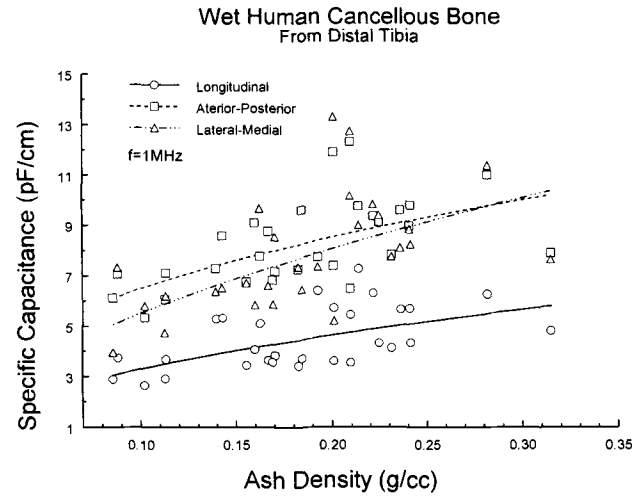

FIGURE 13. The specific capacitance (C_{sp}) as a function of ash density for the longitudinal, anterior-posterior, and lateral medial directions at a frequency of 1 MHZ.

TABLE 4. Linear regression results for the cancellous bone specimens (n = 30) for the specific capacitance (C_{sp}) as a function of density at a frequency of 100 kHZ.

X	Direction	b Intercept	m Slope	r Value	p Value	Fig.
ρ_{wet}	LO	−15.14	23.45	0.6092	<0.001	8
ρ_{wet}	AP	−18.55	33.35	0.5898	<0.001	8
ρ_{wet}	LM	−22.60	36.61	0.5166	<0.01	8
ρ_{dry}	LO	3.60	15.09	0.4887	<0.01	9
ρ_{dry}	AP	6.03	27.59	0.6270	<0.001	9
ρ_{dry}	LM	3.77	32.10	0.5870	<0.001	9
ρ_{ash}	LO	3.93	25.75	0.5337	<0.01	10
ρ_{ash}	AP	7.39	42.97	0.6173	<0.001	10
ρ_{ash}	LM	5.46	49.44	0.5705	<0.001	10

LO, longitudinal; AP, anterior-posterior; LM, lateral-medial.

TABLE 5. Linear regression results for the cancellous bone specimens (n = 30) for the specific capacitance (C_{sp}) as a function of density at a frequency of 1 MHZ.

X	Direction	b Intercept	m Slope	r Value	p Value	Fig.
ρ_{wet}	LO	−6.67	11.00	0.5997	<0.001	11
ρ_{wet}	AP	−6.39	14.43	0.5587	<0.001	11
ρ_{wet}	LM	−9.27	16.81	0.4881	<0.01	11
ρ_{dry}	LO	2.12	7.07	0.4804	<0.01	12
ρ_{dry}	AP	4.51	11.14	0.5505	<0.01	12
ρ_{dry}	LM	2.89	14.61	0.5500	<0.01	12
ρ_{ash}	LO	2.28	12.03	0.5228	<0.01	13
ρ_{ash}	AP	5.02	17.55	0.5486	<0.01	13
ρ_{ash}	LM	3.63	22.64	0.5381	<0.01	13

LO, longitudinal; AP, anterior-posterior; LM, lateral-medial.

TABLE 6. Power regression results for the cancellous bone specimens (n = 30) for the specific capacitance (C_{sp}) as a function of density at a frequency of 100 kHZ.

X	Direction	a Constant	α Exponent	r Value	p Value	Fig.
ρ_{wet}	LO	8.00	2.94	0.6551	<0.0001	8
ρ_{wet}	AP	14.45	2.36	0.6537	<0.0001	8
ρ_{wet}	LM	13.38	2.86	0.5905	<0.0005	8
ρ_{dry}	LO	16.67	0.62	0.5524	<0.0005	9
ρ_{dry}	AP	29.68	0.61	0.6947	<0.0001	9
ρ_{dry}	LM	33.54	0.78	0.6116	<0.0001	9
ρ_{ash}	LO	21.74	0.55	0.5652	<0.0005	10
ρ_{ash}	AP	36.05	0.51	0.6459	<0.0001	10
ρ_{ash}	LM	42.62	0.64	0.5997	<0.0001	10

LO, longitudinal; AP, anterior-posterior; LM, lateral-medial.

TABLE 7. Power regression results for the cancellous bone specimens (n = 30) for the specific capacitance (C_{sp}) as a function of density at a frequency of 1 MHZ.

X	Direction	a Constant	α Exponent	r Value	p Value	Fig.
ρ_{wet}	LO	4.19	2.64	0.6025	<0.0001	11
ρ_{wet}	AP	7.90	1.90	0.5689	<0.0005	11
ρ_{wet}	LM	7.27	2.44	0.5008	<0.001	11
ρ_{dry}	LO	8.10	0.55	0.5172	<0.0005	12
ρ_{dry}	AP	13.68	0.47	0.5892	<0.0005	12
ρ_{dry}	LM	15.85	0.66	0.5816	<0.0005	12
ρ_{ash}	LO	10.26	0.49	0.5581	<0.001	13
ρ_{ash}	AP	16.01	0.39	0.5917	<0.0005	13
ρ_{ash}	LM	19.49	0.55	0.5743	<0.0005	13

LO, longitudinal; AP, anterior-posterior; LM, lateral-medial.

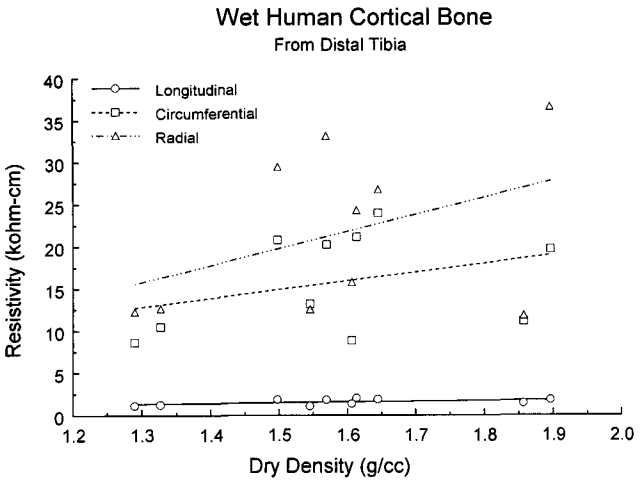

FIGURE 14. The relationship between the resistivity and the dry density in the three orthogonal directions for human cortical bone.

wet density and frequency. The resultant equation for the axial direction was

$$C_{sp} = 72{,}160*f^{-0.72}*\rho_w^{2.25}$$

$$[r = 0.6581, p < 0.001, n = 40]$$

Only the axial direction was used, because the two transverse directions were measured at three frequencies that are not sufficient for the regression analysis.

The electrical properties of cortical bone specimens showed no significant correlations ($p > 0.05$) with density; however, a few possible relationships do merit discussion. Although the cancellous bone samples showed no correlation between the resistivity and density, the cortical bone samples did show a trend for a possible relationship between the resistivity and dry density, as shown in Fig. 14. Similarly, there was a trend for a possible negative correlation between the specific capacitance and dry density, as shown in Fig. 15. The linear regression results between the electrical properties and density of the cortical bone samples are given in Table 8. As shown in Table 8, many of the r values are 0.4 or higher, which could become statistically significant with additional numbers of cortical bone samples.

It has been shown that the mechanical behavior of both cortical and cancellous bone can be modeled treating bone as a single material with varying density (6,7,20,23,24). Therefore, the data for the cancellous and cortical bone were pooled together to examine the possibility of considering bone as a single material with varying density with respect to its electrical behavior. Figure 16 shows the relation between the wet density and the resistivity for the cancellous and cortical data pooled together. The linear and power regression equations are as follows:

$$R_{sp} = -652 + 1{,}147*\rho_w \quad \text{(linear)}$$

$$[r = 0.8794, p < 0.0001, n = 40]$$

$$R_{sp} = 464*\rho_w^{1.79} \quad \text{(power)}$$

$$[r = 0.7976, p < 0.0001, n = 40]$$

Figures 17, 18, and 19 show the specific capacitance as a function of the wet, dry, and ash densities for the axial direction at frequencies of 10 kHZ, 100 kHZ, and 1 MHZ for the combined cancellous and cortical data. The regression results are given in Tables 9 and 10. Although, in general, the linear regression has slightly higher r values, the p values are all less than 0.0001. The exponential values for the power regression are 1.35–2.24 for the wet density, 0.52–0.85 for the dry density, and 0.46–0.75 for the ash density.

DISCUSSION

Several important factors should be considered in the interpretation of the results of this study. All biological tissues exhibit electrical behavior that is temperature dependent (17,31–33,44). The electrical properties of bone also have been shown to vary with age in rats (51). The bone specimens used in this study were taken from individuals who were between 50 and 80 years of age, and, therefore, these properties may vary for specimens taken from younger individuals (51). There is little information available on age-related changes in the electrical properties of bone, and additional studies delineating how age affects the electrical behavior of human bone are warranted. It is believed that a variety of changes, for example, chemical changes, occur in bone with changes in age (19,52). Change in the chemical composition of bone has

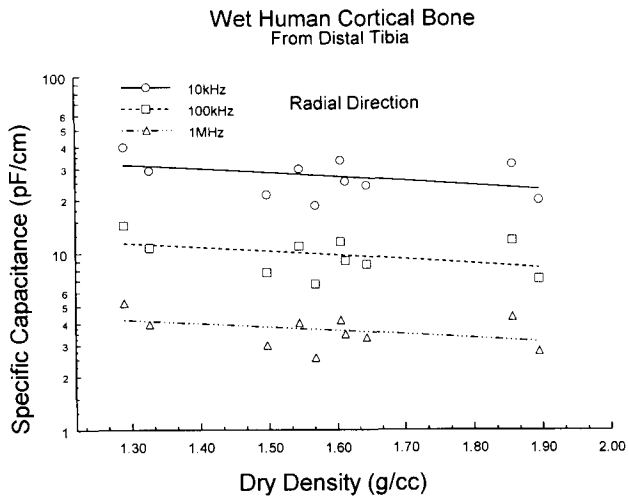

FIGURE 15. The relationship between the specific capacitance and the dry density in the three orthogonal directions for human cortical bone.

TABLE 8. Linear regression results for the cortical bone specimens (n = 10) for the resistivity (R_{sp}) in kΩ cm and the specific capacitance (C_{sp}) as a function of dry density.

Y	Direction	b Intercept	m Slope	r Value	p Value	Fig.
R_{sp} @ 100 kHZ	Axial	0.32	0.78	0.4285	NS	14
R_{sp} @ 100 kHZ	Circumferential	−0.61	10.35	0.3407	NS	14
R_{sp} @ 100 kHZ	Radial	−10.33	20.09	0.4051	NS	14
C_{sp} @ 10 kHZ	Radial	39.90	−8.05	0.2715	NS	15
C_{sp} @ 100 kHZ	Radial	17.87	−5.08	0.4091	NS	15
C_{sp} @ 1 MHZ	Radial	6.34	−1.68	0.4011	NS	15

NS, not significant.

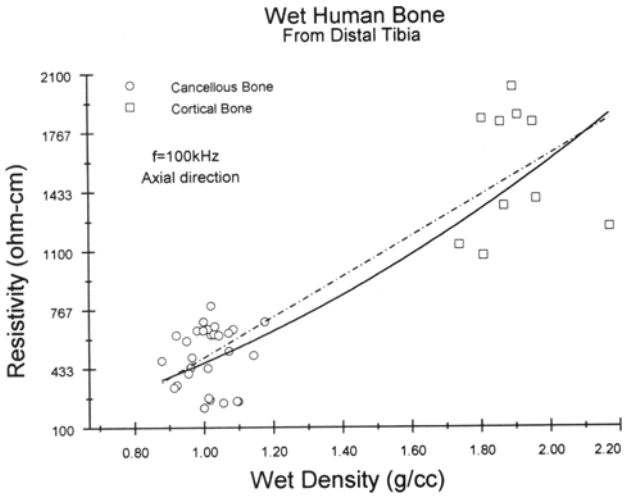

FIGURE 16. The resistivity as a function of wet density in the axial direction for cancellous and cortical bone combined. Both the linear and power curve regression lines are shown.

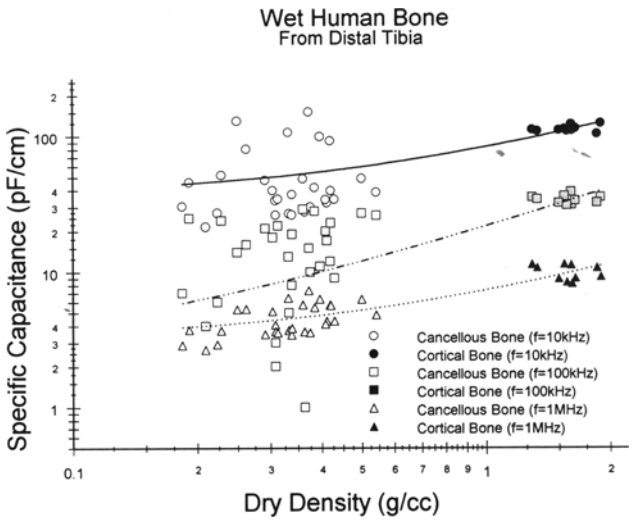

FIGURE 18. The specific capacitance as a function of dry density in the axial direction at frequencies of 10 kHZ, 100 kHZ, and 1 MHZ for cancellous and cortical bone specimens combined.

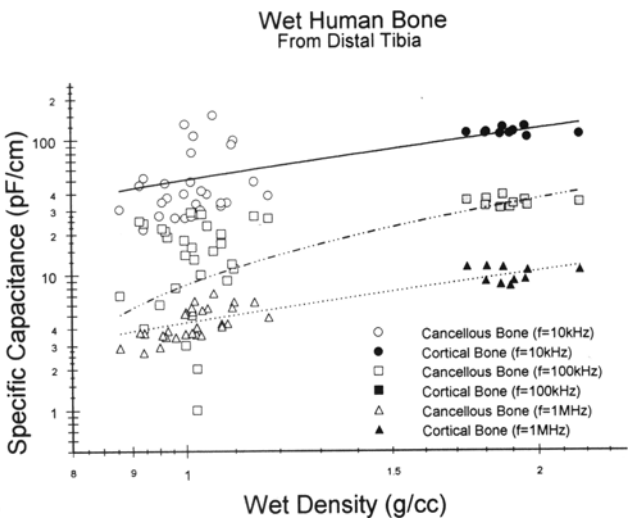

FIGURE 17. The specific capacitance as a function of wet density in the axial direction at frequencies of 10 kHZ, 100 kHZ, and 1 MHZ for cancellous and cortical bone specimens combined.

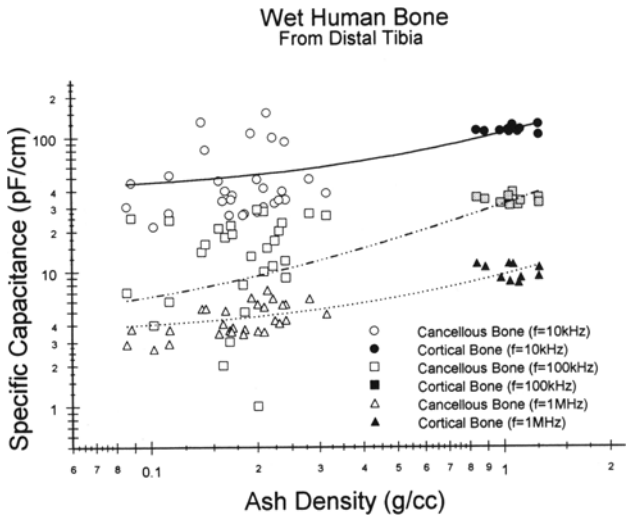

FIGURE 19. The specific capacitance as a function of ash density in the axial direction at frequencies of 10 kHZ, 100 kHZ, and 1 MHZ for cancellous and cortical bone specimens combined.

TABLE 9. Linear regression results for the specific capacitance (C_{sp}) in the axial direction as a function of wet, dry, and ash densities for the cancellous and cortical bone specimens combined (n = 40).

X	Frequency	b Intercept	m Slope	r Value	p Value	Fig.
ρ_{wet}	10 kHZ	−18.34	68.59	0.6821	<0.0001	17
ρ_{wet}	100 kHZ	−19.37	27.78	0.9701	<0.0001	17
ρ_{wet}	1 MHZ	−1.70	6.11	0.9035	<0.0001	17
ρ_{dry}	10 kHZ	35.88	47.11	0.6635	<0.0001	18
ρ_{dry}	100 kHZ	2.34	19.46	0.9637	<0.0001	18
ρ_{dry}	1 MHZ	3.12	4.21	0.8810	<0.0001	18
ρ_{ash}	10 kHZ	39.14	64.63	0.6688	<0.0001	19
ρ_{ash}	100 kHZ	3.77	27.73	0.9637	<0.0001	19
ρ_{ash}	1 MHZ	3.43	5.99	0.8806	<0.0001	19

been shown to affect the streaming potentials (30). We also have observed changes in the electrical properties of demineralized bone (43). The individuals also represented one subpopulation (African-Americans), and there are known physiological differences between the bone of different races (i.e., bone mineral content, bone formation, bone turnover). Therefore, care should be taken in the extrapolation of these data to other populations.

The specimens used in this study were taken from individuals that had some peripheral vascular disease, which may have affected bone circulation; bone circulation, in turn, may have had some effect on the properties of bone tissue, as sometimes is the case for other tissues (12). However, the gangrene portion was only in the distal feet, and the tibia appeared to be normal. In addition, there are different methods by which the density can be determined (47). The use of different methods in measuring the bone density may yield slightly different values, which could affect the results and use of the data (47). In addition, we also have shown that the storage method used can affect the electrical properties of bone (39).

The resistivity of cancellous bone exhibited no correlations with density, but this may not be surprising, because Smith and Foster (50) have shown that the electrical properties of bone marrow vary with the composition of the marrow. This suggests strongly that the conductivity of cancellous bone can change without a change in density. The specific capacitance, however, probably is a function of both the marrow and the bone/marrow interface, which means that a change in density can result in a significant change in specific capacitance. This is shown in Figs. 8–13. The cortical bone is different, because the conductivity of the fluid probably is more consistent, therefore, a relationship between the resistivity and density could exist. However, the small number of data points for the cortical bone may be insufficient to establish the relationship, and a larger number of samples could show a correlation. The same small number of cortical bone samples could be responsible for the lack of significant correlations between the specific capacitance and densities. The results from the combination of both cancellous and cortical bone should be examined with care and caution. This can be demonstrated by studying Figs. 16–19 and by comparing Tables 4–10. As can be seen in Fig. 16, there is some scatter in the cancellous and cortical resistivities, however, because of the number of data points (n = 40) and the large range in density values, the correlations were found, although no correlations were found for only the cancellous bone samples. The slope of 1,147 Ω-cm for the combined cancellous and cortical bone is 47% more than the slope of 780 Ω-cm, as given in Table 8 for cortical bone alone. The exponent for the specific capacitance of cancellous bone at a frequency of 100 kHZ is 2.94 (Table 6), whereas the exponent for the specific capacitance of the cancellous and cortical bone combined at a frequency of 100 kHZ is 2.24 (Table 10).

TABLE 10. Power regression results for the specific capacitance (C_{sp}) in the axial direction as a function of wet, dry, and ash densities for the cancellous and cortical bone specimens combined (n = 40).

X	Frequency	a Constant	α Exponent	r Value	p Value	Fig.
ρ_{wet}	10 kHZ	43.11	1.50	0.6914	<0.0001	17
ρ_{wet}	100 kHZ	8.07	2.24	0.9496	<0.0001	17
ρ_{wet}	1 MHZ	4.24	1.35	0.8796	<0.0001	17
ρ_{dry}	10 kHZ	82.94	0.55	0.6540	<0.0001	18
ρ_{dry}	100 kHZ	22.01	0.85	0.9401	<0.0001	18
ρ_{dry}	1 MHZ	7.76	0.52	0.8760	<0.0001	18
ρ_{ash}	10 kHZ	104.57	0.49	0.6665	<0.0001	19
ρ_{ash}	100 kHZ	31.15	0.75	0.9438	<0.0001	19
ρ_{ash}	1 MHZ	9.60	0.46	0.8832	<0.0001	19

There are three basic questions or issues with regard to the data presented. The first issue is whether the relationship between the electrical properties and densities more likely is a linear or power law relationship. Tables 4–10 indicate that the power law fit could be more likely for the cancellous bone, which would be similar to what Carter and Hayes found for mechanical properties (6,7). However, for the cortical bone, the lack of sufficient numbers prevents any conclusion, and the pooled results for the cancellous and cortical bone combined also are not clear. The second issue is one of the similarity and difference between the mechanical and electrical behaviors of bone. The bone marrow is not necessarily important to the mechanical behavior of bone (6,7,20), but, it is very important for the electrical behavior of bone (40). Both the mechanical and electrical properties are influenced by the bone structure (8,20,23–25); however, the relationship between the electrical behavior of bone and its structure is not well known, and it is likely to be different from that between the mechanical behavior and structure. Finally, the third issue is whether bone can be considered electrically as a single material with varying density, as is the case with the mechanical properties, must be examined further. Although there appear to be similarities between the electrical and mechanical behaviors of bone tissues, there also are major differences. In Figs. 16–19, it may appear that bone tissue could be considered electrically as a single material of varying densities, although this should be undertaken with caution, particularly concerning the resistivity.

In summary, we have demonstrated that knowing the density of the bone may make it possible to estimate the electrical properties of the bone tissue. Although this study does provide data that suggest that estimation of the electrical properties from the density is possible, there are concerns, and additional work is needed before any conclusions can be reached. These data and results, along with additional work, can help in better understanding the electrical behavior of whole bone and the electrical field and current distributions under various electrical stimulation conditions. Recently, FEM has been initiated along this direction (16). A more accurate characterization of the electrical properties of bone will improve our understanding of the electrical behavior of bone and will contribute to a more accurate modeling of bone tissue. Moreover, bone density often is reduced with various disease processes (*i.e.*, osteoporosis). Therefore, if electrical stimulation is to be used as a treatment modality, we must determine the relationship between the bone density and its electrical properties so that appropriate stimulation parameters can be selected to produce suitable current densities. Additional work is in progress in our laboratory regarding the dependence of the electrical and dielectric properties on the apparent densities and microstructure of the bone.

REFERENCES

1. Bassett, C. A. L., S. N. Mitchell, and S. R. Gaston. Treatment of ununited tibial diaphyseal fractures with pulsing electromagnetic fields. *J. Bone Joint Surg.* 63-A(4):511–523, 1981.
2. Bassett, C. A. L., A. A. Pilla, E. I. Mitchell, and R. E. Booth. Repair of non-unions by pulsing electromagnetic fields. *Acta Ortho. Belgica* 44:706–724, 1978.
3. Brighton, C. T., Z. B. Friedenberg, E. I. Mitchell, and R. E. Booth. Treatment of nonunion with constant direct current. *Clin. Orthop.* 124:106–123, 1977.
4. Brighton, C. T., G. T. Tadduni, S. R. Goll, and S. R. Pollack. Treatment of denervation/-disuse osteoporosis in the rat with a capacitively coupled electrical signal: effects of bone formation and bone resorption. *J. Orthop. Res.* 6(5): 676–684, 1988.
5. Cappanna, R., D. Donati, C. Masetti, M. Manfrini, A. Panozzo, R. Cadossi, and M. Campanacci. Effect of electromagnetic fields on patients undergoing massive bone grafts following bone tumor resection. *Clin. Orthop. Rel. Res.* 306:213–221, 1994.
6. Carter, D. R., and W. C. Hayes. Bone compressive strength: the influence of density and strain rate. *Science* 194:1174–1176, 1976.
7. Carter, D. R., and W. C. Hayes. The compressive behavior of bone as a two-phase porous structure. *J. Bone Joint Surg.* 59-A:954–962, 1977.
8. Chakkalakal, D. A., and M. W. Johnson. Electrical properties of compact bone. *Clin. Orthop. Rel. Res.* 161:133–145, 1981.
9. Chakkalakal, D. A., M. W. Johnson, R. A. Harper, and J. L. Katz. Dielectric properties of fluid-saturated bone. *IEEE Trans. Biomed. Eng.* 27(2):95–100, 1980.
10. Chen, I. I. H., and S. Saha. Analysis of current distribution in bone produced by pulsed electro-magnetic field stimulation of bone. *Biomat. Art. Cells Art. Org.* 15(4):737–744, 1988.
11. Cundy, P. J., and D. C. Paterson. A ten-year review of treatment of delayed union with an implanted bone growth stimulator. *Clin. Orthop.* 259:216–222, 1990.
12. Davies, R. J., J. Renah, D. Kaplan, R. D. Juncosa, C. Pempinello, H. Asburn, and M. M. Sedwitz. Epithelial impedance analysis in experimentally induced colon cancer. *Biophys. J.* 52:783–790, 1987.
13. De Mercato, G., and F. J. Garcia-Sanchez. Dielectric properties of fluid-saturated bone: a comparison between diaphysis and epiphysis. *Med. Biol. Eng. Comput.* 26:313–316, 1988.
14. De Mercato, G., and F. J. Garcia-Sanchez. Variation of the electric properties along the diaphysis of bovine femoral bone. *Med. Biol. Eng. Comput.* 29:441–446, 1991.
15. De Mercato, G., and F. J. Garcia-Sanchez. Correlation between low-frequency electric conductivity and permittivity in the diaphysis of bovine femoral bone. *IEEE Trans. Biomed. Eng.* 39:523–525, 1992.
16. Ducheyne, P., L. Y. Ells, S. R. Pollack, D. Pienkowski, and J. M. Cuckler. Field distributions in the rat tibia with and without a porous implant during electrical stimulation: a parametric modeling. *IEEE Trans. Biomed. Eng.* 39(11): 1168–1178, 1992.
17. Geddes, L. A., and L. E. Baker. The specific resistance of biological material: a compendium of data for the biomed-

ical engineer and physiologist. *Med. Biol. Eng.* 5:271–293, 1967.
18. Gong, J. K., J. S. Arnold, and S. H. Cohn. Composition of trabecular and cortical bone. *Anat. Rec.* 149:325–332, 1964.
19. Hancox, N. M. *Biology of Bone*. London: Cambridge University, 1972, pp. 24–49.
20. Hayes, W. C. Biomechanics of cortical and trabecular bone: implications for assessment of fracture risk. In: *Basic Orthopaedic Biomechanics*, edited by V. C. Mow and W. C. Hayes. New York: Raven Press, 1991, pp. 93–142.
21. Heppenstall, R. B. Constant direct-current treatment for established nonunion of the tibia. *Clin. Orthop. Rel. Res.* 178:179–184, 1983.
22. Huiskes, R. Biomechanics of artificial-joint fixation. In: *Basic Orthopaedic Biomechanics*, edited by V. C. Mow and W. C. Hayes. New York: Raven Press, 1991, pp. 375–442.
23. Kaplan, F. S., W. C. Hayes, T. M. Keaveny, A. Boskey, T. A. Einhorn, and J. P. Iannotti. Form and function of bone. In: *Orthopedic Basic Science*, edited by S. R. Simon. Rosemont, IL: American Academy of Orthopedic Surgery, 1994, pp. 172–189.
24. Keyak, J. H., I. Y. Lee, and H. B. Skinner. Correlations between orthogonal mechanical properties and density of trabecular bone: use of different densitometric measures. *J. Biomed. Mat. Res.* 28:1329–1336, 1994.
25. Kosterich, J. D., K. R. Foster, and S. R. Pollack. Dielectric permittivity and electrical conductivity of fluid saturated bone. *IEEE Trans. Biomed. Eng.* 30(2):81–86, 1983.
26. Kosterich, J. D., K. R. Foster, and S. R. Pollack. Dielectric properties of fluid-saturated bone—the effect of variation in conductivity of immersion fluid. *IEEE Trans. Biomed. Eng.* 31(4):369–373, 1984.
27. Lakes, R. S., R. A. Harper, and J. L. Katz. Dielectric relaxation in cortical bone. *J. Appl. Phys.* 48:808–811, 1977.
28. Liboff, A. R., R. A. Rinaldi, L. S. Lavine, and M. H. Shamos. On electrical conduction in living bone. *Clin. Orthop.* 106:330–335, 1975.
29. Martin, R. B. Comparison of capacitive and inductive bone stimulation devices. *Ann. Biomed. Eng.* 7:387–409, 1979.
30. Otter, M., S. Goheen, and W. S. Williams. Streaming potentials in chemically modified bone. *J. Orthop. Res.* 6: 346–359, 1988.
31. Pethig, R. *Dielectric and Electronic Properties of Biological Materials*. New York: John Wiley & Sons, 1979, 376 pp.
32. Pethig, R. Dielectric properties of body tissues. *Clin. Phys. Physiol. Meas.* 8:5–12, 1987.
33. Pethig, R., and D. B. Kell. The passive electrical properties of biological systems: their significance in physiology, biophysics, and biotechnology (review article). *Phys. Med. Biol.* 32(8):933–970, 1987.
34. Reddy, G. N., and S. Saha. A differential method for measuring impedance properties of bone. *J. Bioelec.* 1(2):173–194, 1982.
35. Reddy, G. N., and S. Saha. Electrical and dielectric properties of wet bone as a function of frequency. *IEEE Trans. Biomed. Eng.* 31:296–302, 1984.
36. Reinish, G. B., and A. S. Nowick. Effect of moisture on the electrical properties of bone. *J. Electrochem. Soc.* 123(10):1452–1455, 1976.
37. Rubin, C. T., K. J. McLeod, and L. E. Lanyon. Prevention of osteoporosis by pulsed electromagnetic fields. *J. Bone Joint Surg.* 71-A(3):411–417, 1989.
38. Saha, S., G. N. Reddy, and J. A. Albright. Factors affecting the measurement of bone impedance. *Med. Biol. Eng. Comput.* 22:123–129, 1984.
39. Saha, S., and P. A. Williams. Effect of various storage methods on the dielectric properties of compact bone. *Med. Biol. Eng. Comput.* 26:199–202, 1988.
40. Saha, S., and P. A. Williams. Electric and dielectric properties of wet human cancellous bone as a function of frequency. *Ann. Biomed. Eng.* 17:143–158, 1989.
41. Saha, S., and P. A. Williams. Electric and dielectric properties of wet human cortical bone as a function of frequency. *IEEE Trans. Biomed. Eng.* 39:1298–1304, 1992.
42. Saha, S., and P. A. Williams. Comparison of the electrical and dielectric behavior of wet human cortical and cancellous bone tissue from the distal tibia. *J. Orthop. Res.* 13:524–532, 1995.
43. Saha, S., P. A. Williams, D. V. Rai, and J. A. Albright. Electrical properties of demineralized bone. Digest of Papers, Eighth Southern Biomedical Engineering Conference, pp. 147, 1989 (abstract in *Biomat. Artif. Cells Artif. Organs* 17(4):456, 1989).
44. Schwan, H. P. Dielectric properties of cells and tissues. In: *Interactions Between Electromagnetic Fields and Cells*, edited by A. Chiabrera, C. Nicolini, and H. P. Schwan, New York: Plenum Press, 1985, XXX pp.
47. Sharrard, W. J. W. A double-blind trial of pulsed electromagnetic fields for delayed union of tibial fractures. *J. Bone Joint Surg.* 72-B(3):347–355, 1990.
46. Singh, S., and J. Behari. Frequency dependence of electrical properties of human bone. *J. Bioelec.* 3:347–356, 1984.
47. Singh, S., and S. Saha. Bone density measurements: a preliminary study. Biomedical Engineering III Recent Developments, Proceedings of the Third Southern Biomedical Engineering Conference, 1984, pp. 79–81.
48. Singh, S., and S. Saha. Electrical properties of bone: a review. *Clin. Orthop. Rel. Res.* 186:249–271, 1984.
49. Skerry, T. M., M. J. Pead, and L. E. Lanyon. Modulation of bone loss during disuse by pulsed electromagnetic fields. *J. Orthop. Res.* 9(4):600–608, 1991.
50. Smith, S. R., and K. R. Foster. Dielectric properties of low-water-content tissues. *Phys. Med. Biol.* 30(9):965–973, 1985.
51. Swanson, G. T., and J. F. Lafferty. Electrical properties of bone as a function of age, immobilization, and vibration. *J. Biomech.* 5:261–266, 1972.
52. Timmins, P. A., and J. C. Wall. Review: bone water. *Calcif. Tiss. Res.* 23:1–5, 1977.
53. Woo, J. W., P. Hua, J. G. Webster, and W. J. Tompkins. Measuring lung resistivity using electrical impedance tomography. *IEEE Trans. Biomed. Eng.* 39:756–760, 1992.
54. Yorkey, T. J., J. G. Webster, and W. J. Tompkins. Comparing reconstruction algorithms for electrical impedance tomography. *IEEE Trans. Biomed. Eng.* 34:843–852,1987.